Electronic Supplementary Material (ESI) for ChemComm.

Electronic Supplementary Information

Shaping Metal-Organic Framework Materials with A Honeycomb Internal Structure

Yingya Zhang, Juanjuan Cai, Dayou Zhang, Xuebin Ke*, and Lixiong Zhang*

Abstract: The large-scale use of crystalline nanomaterials in industry demands an economical approach to handle these materials at a macroscopic scale. Current methods to mould powders into shaped geometries have some unavoidable drawbacks, such as low nanoparticle loads and difficulties to create complex morphologies or ordered porosity. Herein a self-assembly technology is proposed to fabricate hierarchical porous materials. This simple and efficient strategy allows ZIF-8 nanocrystals to constitute a honeycomb internal structure while shaped into millimeter-scale spheres through solidification of chitosan (CS). The specific surface area is 1309 m^2/g with ZIF-8 loads up to 83 wt%. This fabrication can be expanded to other morphologies (fibers) or porous materials, such as ZIF-7 and ZIF-67, and achieves similar structures while using different metal ions or ligand molecules. This engineering approach is potentially transformative for industrial manufacturing of crystalline nanomaterials.

Table of Contents

Section 1 Experimental procedures

1.1 ZIF-8/CS microspheres

ZIF-8/CS microspheres were prepared by impregnation-gelation-hydrothermal technique. Typically, 0.6 g (2 mmol) of zinc nitrate hexahydrate was dissolved in 10 g of 2.0 wt% chitosan solution consisting of 2.0 g chitosan, 94.8 g deionized water, and 3.2 ml acetic acid (36 wt%). 2.0 g NaOH and 2.6 g 2-Methylimidazole (Hmim) were dissolved in 35.4 g deionized water, making the NaOH and Hmim contents of 5 wt% and 6.6 wt%, respectively. Then 8.2 g of the Zn^{2+}-chitosan solution was added to 40 g of the mixture solution of NaOH and Hmim through a stainless steel needle (inner diameter, 0.26 mm), which use a syringe pump (LSP01-1BH, Longer) and set at 10 ml/min (Figure S1). Microspheres were immediately formed. They were left at 80 °C for 12 hours. ZIF-8/CS microspheres were obtained after filtrating, washing and freeze-drying.

ZIF-8/CS hybrid microspheres can be prepared with different ZIF-8 loads by changing the concentration of Zn(NO$_3$)$_2$ and Hmim,. The maximum concentration of Zn(NO$_3$)$_2$ in 2 wt% chitosan solution is 5.2 wt% at room temperature, which limits ZIF-8 loads to 83 wt%.

The similar strategies and conditions were applied to preparating ZIF-67/CS microspheres while 3.5 wt% of Co(NO$_3$)$_2$ in 2 wt% chitosan solution was used. For the preparation of ZIF-7/CS microspheres, 8.2 g of Zn^{2+}-chitosan solution was dropped to 40 g of the mixture solution composed of 5 wt% NaOH and 3.87 wt% benzimidazol. Afterward, they were left for 36 hours. Finally, ZIF-7/CS hybrid microspheres were obtained after filtrating, washing and freeze-drying.

1.2 ZIF-8/CS hybrid fibers

The ZIF-8/CS hybrid fibers were prepared using a homemade co-axle microfluidic setup (Fig. S1b). The Zn^{2+}-chitosan solution and a mixture solution of NaOH and Hmim acted as continuous phase and dispersed phase, respectively, which were supplied by two syringe pumps set at each flow rate of 3 ml/minute. The fiber was immediately formed in the PTFE tube and spun out of the tube. It was collected with the excessive solution in a container, which was hereafter heated to 80 °C in an oven for 12 hours for ZIF-8 growth. ZIF-8/CS hybrid fibers were obtained after filtrating, washing and freeze-drying.

1.3 Cu(II) adsorption of the ZIF-8/CS composites.

The ZIF-8/CS composites were heated in 150 ^{o}C for 4 hours before testing. The ZIF-8/CS hybrid materials with different morphologies, including microsphere, hemisphere, fiber with length varied from 0.5 mm to 3.0 mm, were tested for Cu(II) adsorption under the same condition for comparison. In general, 0.1 g of the ZIF-8/CS composite was placed in 300 ml of 200 ppm copper chloride aqueous solution under stirring at room temperature. The residual Cu(II) concentration in the mother liquid was measured at different adsorption durations by inductively coupled plasma atomic emission spectroscopy (ICP-AES, Optima 2000DV). For measuring residual Cu(II) concentration, about 3 ml of the mother liquid was taken out for ICP by a springe equipped with a microfiltration filter in case of any ZIF-8 crystals retained in the sample. After sampling, identical amounts of deionized water were added to the system to maintain the constant quantity of liquid phase.

1.4 Characterization

X-ray diffraction (XRD) patterns were collected on a Bruker D8 Advance powder diffractometer using Ni-filtered Cu Ka radiation source at 40 kV and 100 mA. The scan rate is 5 °/min with a step size of 0.02°. The samples were prepared by grounding. Scanning electron microscope (SEM, Hitachi S-4800) was used to investigate the microstructure of the samples. The Fourier transform infrared (FT-IR) spectra were obtained on the Nexus 870 FT-IR spectrometer. Samples were mixed and grounded with KBr (in a mass ratio of 1:10) for FT-IR measurement in the wavenumber range of 4000-400 cm^{-1}. Thermogravimetric analysis (TGA, Netzsch STA 409) was performed in air at a heating rate of 10 °C/min to 600 °C. N$_2$ adsorption–desorption measurements were performed at 77 K on Micromeritics ASAP 2020 instrument. The samples were all outgassed at 150 ^{o}C for 4 h prior to analysis. The total pore volume was evaluated at a relative pressure of about 0.99 and the specific surface areas were determined by the Brunauer-Emmett-Teller (BET) method.

Section 2 Fabrication devices for microspheres and fibers.

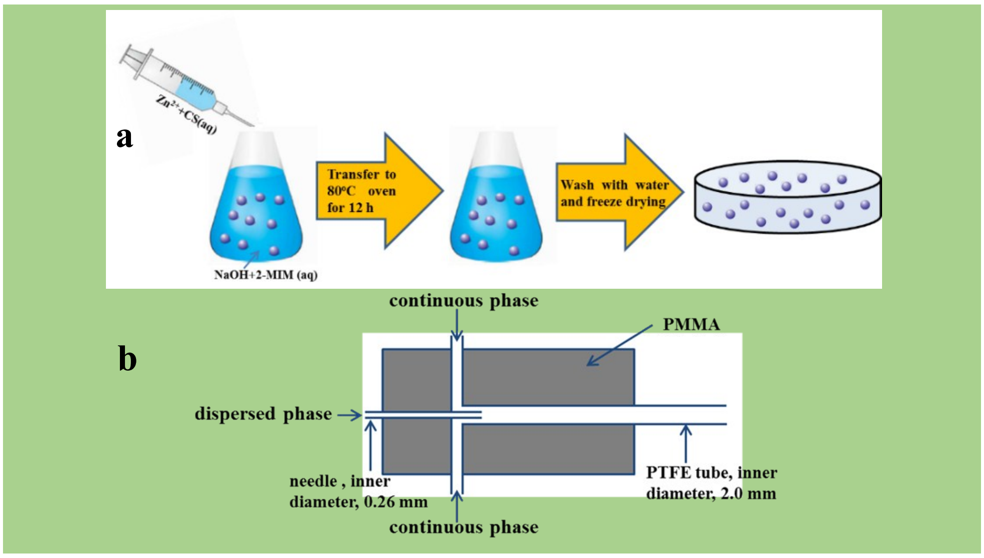

Figure S1 Schematic process for the preparation of ZIF-8/CS hybrid microspheres (a) and microfluidic setup for synthesizing ZIF-8/CS fibers (b).

Section 3 Fabrication of ZIF-8/CS microspheres.

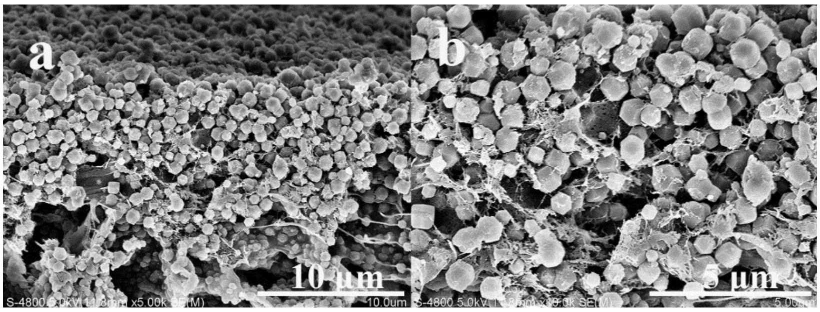

Figure S2 SEM images of ZIF-8/CS microspheres obtained from the typical synthesis. (a) cross-section closed to the outer surface; (b) outer surface.

Figure S3 shows XRD patterns and FT-IR spectra of the samples prepared in the typical synthesis. The XRD patterns confirm a high crystallinity of ZIF-8/CS microspheres and the FT-IR spectra reveal characteristic absorption bands assigned to chitosan and ZIF-8 crystals.[1] The broad band at 3482 cm^{-1}, corresponding to the stretching vibration of hydroxyl, amino and amide groups in chitosan, shifts to 3440 cm^{-1}, whicih indicates the formation of hydrogen bonds between the -NH_2 radicals of ZIF-8 and chitosan. The bands at 1653 cm^{-1} and 1598 cm^{-1} assigned to amide groups in chitosan indicate strong interactions between amide groups and zinc ions of ZIF-8. The sharp peak at 421 cm^{-1} related to Zn–N banding is ascribed to the introduction of ZIF-8 crystals. [1,2]

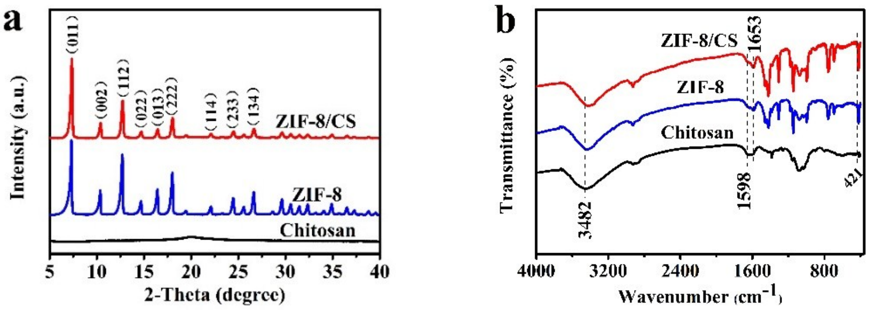

Figure S3 XRD patterns (a) and FT-IR spectra (b) of ZIF-8, ZIF-8/CS microspheres and chitosan.

We conduct TG analysis to determine the ZIF-8 loading amounts, compared to CS and ZIF-8 prepared under the same procedure (Figure S4a). As CS is completely burnt-off and ZIF-8 has a residual of 35.4 % at 600 °C, the ZIF-8 loads in the ZIF-8/CS microspheres can be estimated to be 68 % according to the residue of 24.1 %. Nitrogen adsorption-desorption isotherm of the hybrid exhibits a typical type I isotherm (Figure S4b). The specific surface area is 1076 m^2 g^{-1} with a pore volume of 425.3 cm^3 g^{-1}. As the specific surface area of CS microspheres is only 7.4 m^2 g^{-1}, we can estimate the surface area of ZIF-8 is 1580 m^2 g^{-1}. [3] We also test the CO_2 adsorption isothermal of the ZIF-8/CS microspheres at 25 °C. The result indicates that the CO_2 adsorption amount at 101 kPa is 0.57 mmol/g and equivalent to 0.84 mmol/g of pure ZIF-8, which is comparable to the reported results.[4] The ZIF-8/CS composites reveals that we can assemble ZIF-8 nanocrystals into the shaped microspheres/fibers, without deteriorating the physical property of ZIF-8 crystals themselves.

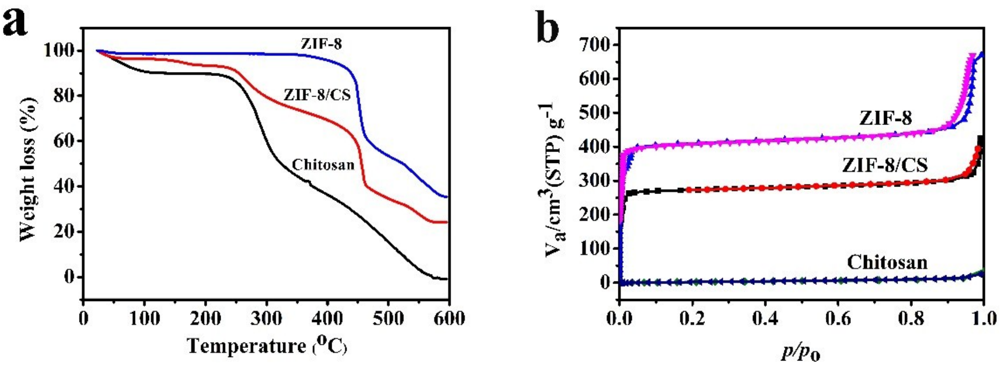

Figure S4 TG curves (a) and nitrogen adsorption-desorption isotherms (b) of ZIF-8, ZIF-8/CS microspheres and chitosan.

[1] a) Park, K. S.; Ni, Z.; Cote, A. P.; Choi, J. Y.; Huang, R.; Uribe-Romo, F. J.; Chae, H. K.; O'Keeffe, M.; Yaghi, O. M. *Proc. Nat. Acad. Sci. USA*. **2006**, *103*, 10186-10191; b) Hu, Y.; Kazemian, H.; Rohani, S.; Huang, Y.; Song, Y. *Chem. Commun*. **2011**, *47*, 12694-12696.

[2] a) Gao, X.; Xiao, H.; Baigude, H.; Guan, W.; Liu, Z. *Sci. Rep*. **2016**, *6*, 37705; b) Han, Y.; Qi, P.; Li, S.; Feng, X.; Zhou, J.; Li, H.; Su, S.; Li, X.; Wang, B. *Chem. Commun*. **2014**, *50*, 8057-8060.

[3] Moosa, A.; Ridha, A. M.; Kadim, A. *Am. J. Mater. Sci.* **2016**, *6*, 95-104.

[4] Kontos, G.; Likodimos, V.; Veziri, C. M.; Kouvelos, E.; Moustakas, N.; Karanikolos, G. N.; Romanos, G. E. *Chemsuschem*. **2014**, *7*, 1696-1702.

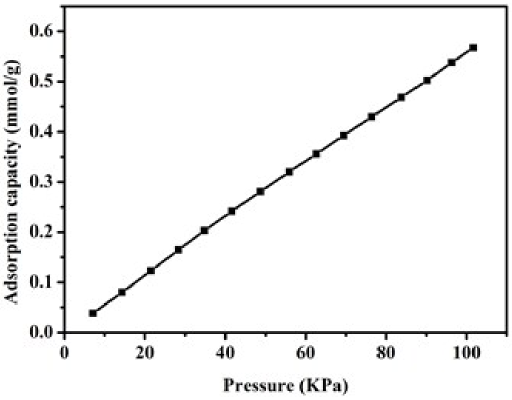

Figure S5 CO_2 adsorption isotherms of ZIF-8/CS microspheres at room temperature.

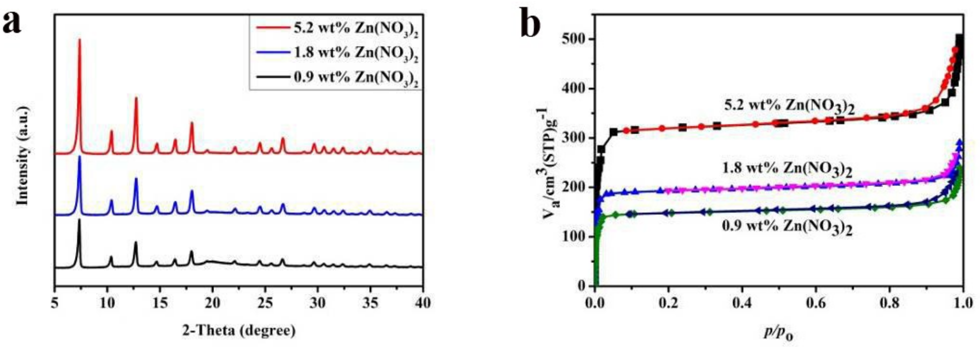

Figure S6 (a) XRD patterns, and (b) N_2 absorption-desorption isotherms of ZIF-8/CS microspheres obtained from the concentration of $Zn(NO_3)_2$ from 0.9 wt% to 5.2 wt%.

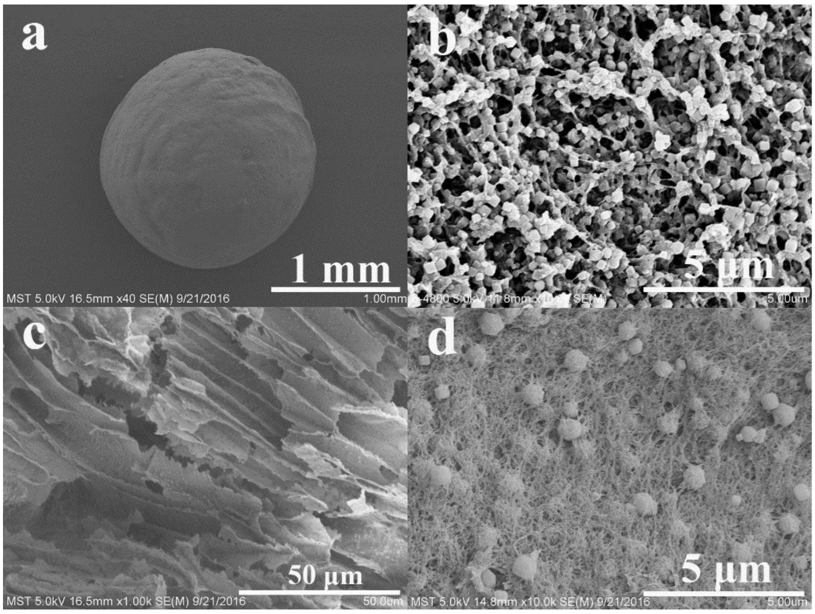

Figure S7 SEM images of the ZIF-8/CS microspheres prepared with the $Zn(NO_3)_2$ concentration of 0.45 wt%. (a) The overall view, (b) outer surface, (c) cross-section, and (d) surface of the channel.

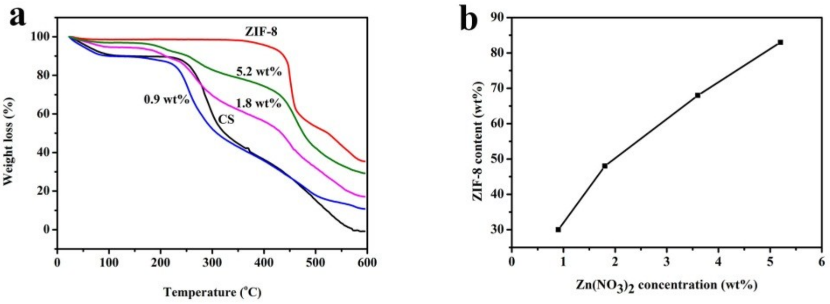

Figure S8 (a)TG analysis of ZIF-8/CS microspheres obtained from the concentration of $Zn(NO_3)_2$ from 0.9 wt% to 5.2 wt% and (b) the relationship between the ZIF-8 contents and $Zn(NO_3)_2$ concentrations in the ZIF-8/CS microspheres.

Section 4 Synthesis of the ZIF-8/CS hybrid fibers

The surface of the fiber is comprised of chitosan and ZIF-8 particles, with the increased numbers and densities as increased $Zn(NO_3)_2$ amount used (Fig. S7 and Fig. S8a-c). The cross-section of the fiber shows a core/shell and cellular structure, slightly different from the inner structure of the microspheres (Fig. S7). Generally, a three-layer structure is formed, with the layers around the surface and the center being dense, and the middle layer being porous and composed of axial-oriented channels. However, the shape of the channel is irregular. The inner structure changes with the amount of $Zn(NO_3)_2$ used. The core is composed of interconnected sheets and dense chitosan fibril when 1.8 wt% and 5.2 wt% of $Zn(NO_3)_2$ are used, respectively. Especially, the core is hollow when the $Zn(NO_3)_2$ content is 3.6 wt% (Fig. S7b).

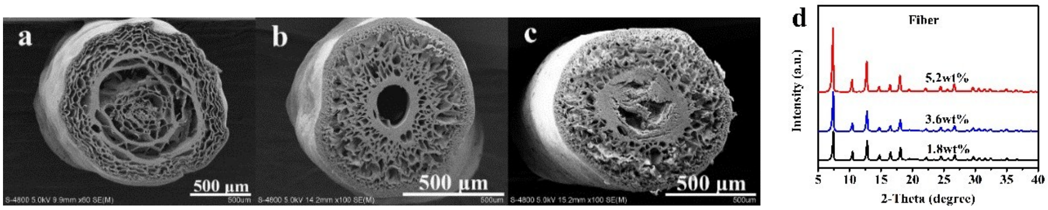

Fig. S9 Cross-section images of ZIF-8/CS fiber prepared with different $Zn(NO_3)_2$ concentration. (a) 1.8 wt%, (b) 3.6 wt%, (c) 5.2 wt%. (d) XRD patterns of ZIF-8/CS hybrid fiber.

Section 5 Formation mechanism of honeycomb-structured ZIF-8/CS hybrid microspheres

To explore the function of Zn^{2+} in the formation of the honeycomb structure, we observe the structure evolution of CS with the same procedure but without Zn^{2+} addition. No uniform porous structures are formed in CS microspheres alone (Figure S10a), while honeycomb porous networks present in Zn^{2+}/CS microspheres which have $Zn(NO_3)_2$ content of 1.8 wt% or lower (Figure S10b-e). When the $Zn(NO_3)_2$ content is up to 3.6 wt%, the formed structures are different from honeycomb (Figure S10f-g). These results indicate that the small amounts of Zn^{2+} are necessary to assemble a uniform honeycomb porous structure. The interaction between Zn^{2+} and CS makes a great contribution. Chitosan can be protonated by acetic acid, and adsorb Zn^{2+} by ion-exchange to form the metal-chitosan complex.[5] Such complex can be solidified to form microspheres in alkaline conditions. During this process, rearrangement of chitosan occurs and forms a cellular porous structure (Figure S10h-i). Such porous structure becomes uniform and stable after freeze-drying, possibly ascribed to the ice-template mechanism.[6] Therefore, the interaction between Zn^{2+} and chitosan, assembly of Zn^{2+}-chitosan complex, and freeze-drying all contribute to the formation of a stable cellular porous structure. The subsequent reaction of Zn^{2+} with Hmim does not have significant influence on the porous structure. A high Zn^{2+} content may hinder the formation of cellular structure in the case that no sufficient Hmim presents in the solution (Figure S10f). However, with Hmim addition, those preparations at high Zn^{2+} contents can still proceed to obtain honeycomb inner structures, possibly due to the fast reaction between Zn^{2+} and Hmim, which consumes the Zn^{2+} ions remarkably.

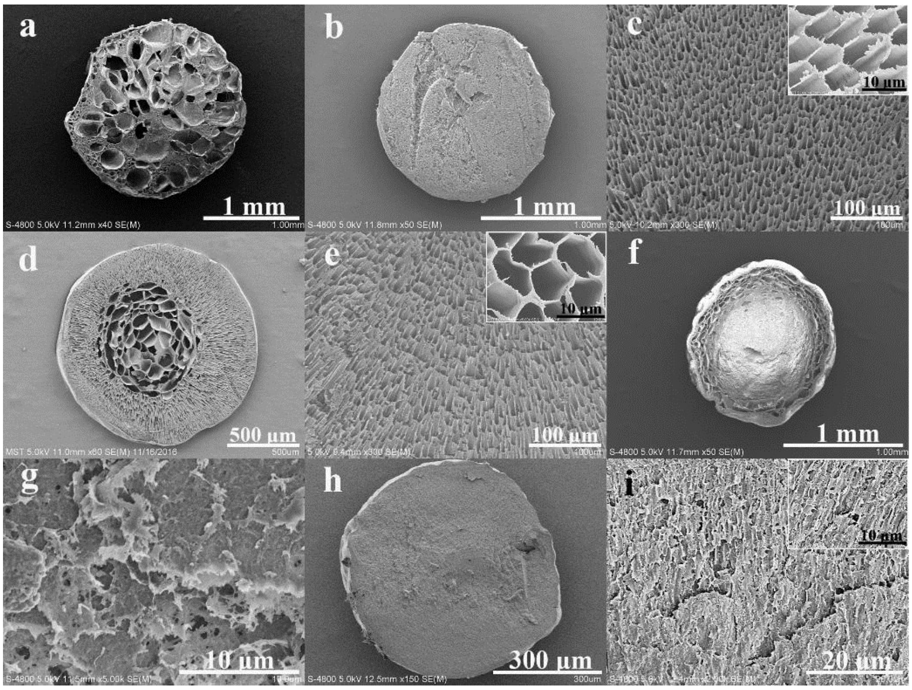

Figure S10 SEM images of the CS microsphere prepared with different $Zn(NO_3)_2$ contents. (a) 0 wt%, (b-c) 0.9 wt%, (d-e) 1.8 wt%, (f-g) 3.6 wt%, and (h-i) 0.9 wt%. The samples (h-i) are dried at room temperature after extracting water using methanol. The insets in (c), (e) and (i) are high-resolution images.

[5] Liu, X.; Hu, Q.; Fang, Z.; Zhang, X.; Zhang, B. *Langmuir* **2009**, *25*, 3-8.

[6] Gutiérrez, M. C.; Ferrer, M. L.; Monte, F. D. *Chem. Mater.* **2008**, *20*, 634-648.

Section 6 Synthesis of the ZIF-7/CS and ZIF-67/CS composites

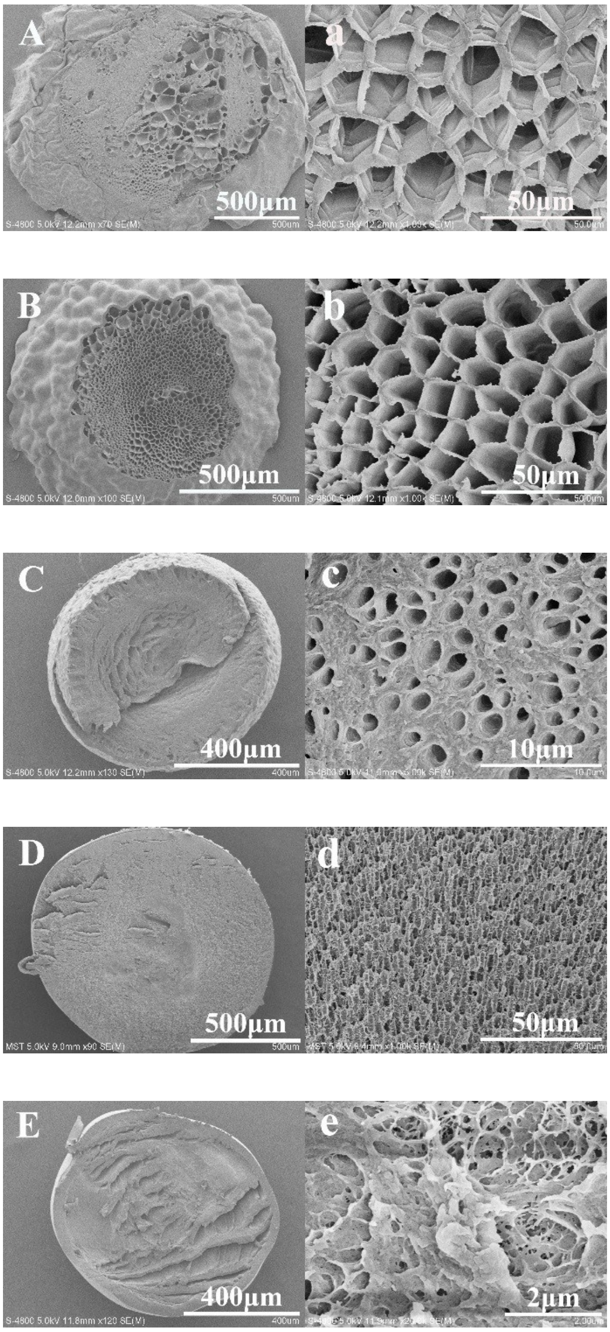

Figure S11 SEM images of microspheres prepared by dropping 0.9 wt% metal ion-2wt% chitosan solution in 5 wt% NaOH solution and freeze-drying. The microspheres were cut into half for SEM observation. The images reveal that when Ca^{2+}（a）, Fe^{3+}（b）, Ni^{2+} （c） and Co^{2+}（d） are used, internal honeycomb porous structure is formed in the chitosan microspheres. When Cu^{2+} （e） is used, there is no formation of such honeycomb pores in the chitosan microspheres.

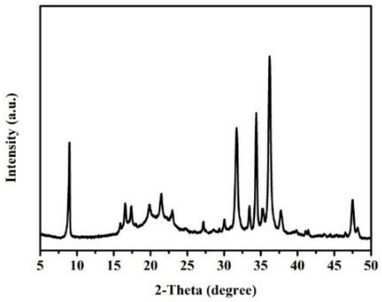

Figure S12 The XRD pattern of the ZIF-7/CS hybrid microspheres.

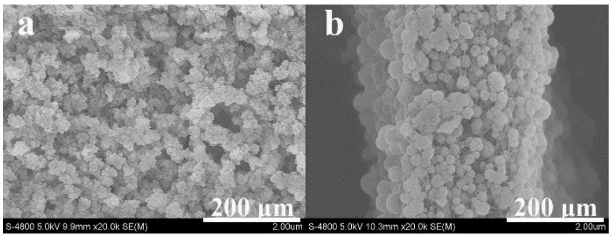

Figure S13 SEM images of ZIF-7/CS hybrid microspheres. (a) outer surface, (b) the wall between adjacent channels.

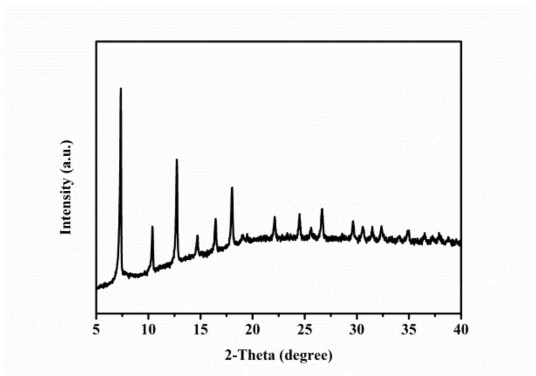

Figure S14 The XRD pattern of the ZIF-67/CS hybrid microspheres.

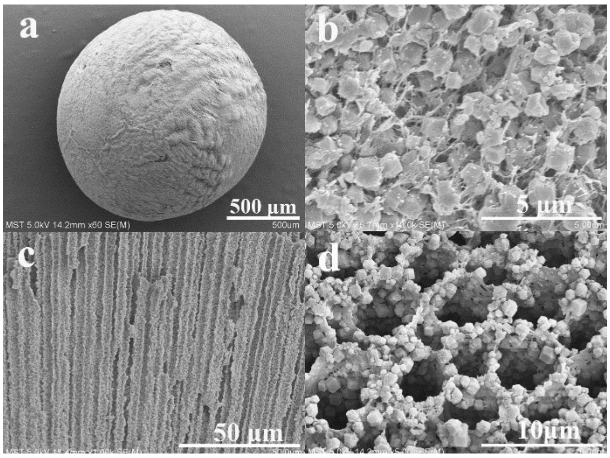

Figure S15 SEM images of ZIF-67/CS hybrid microspheres. (a) overall view, (b) outer surface, (c) cross-section, (d) channel structure.